9th INTERNATIONAL SYMPOSIUM ON MEASUREMENT AND QUALITY CONTROL (9th ISMQC)
November 21-24, 2007, IIT Madras

FUNDAMENTAL STUDY FOR DEVELOPING THE NANO-CMM WITH A MICRO PROBE BASED ON OPTICAL FORCE DYNAMICS

Takaya Y.
Dept. of Mechanical Engineering, Graduate School of Engineering, Osaka University
2-1 Yamadaoka Suita, Osaka, 565-0871 JAPAN
takaya@mech.eng.osaka-u.ac.jp

Abstract: *In this paper, the dynamic properties of the optically vibrated microprobe for establishing the nano-CMM are presented. The principle of the position detection probe is based on the single-beam gradient-force optical trap of a micrometer size probe sphere and the vibration probing technique. A novel principle of position sensing using the phase delay response due to drastically increasing viscous drag coefficients near the surface is proposed. Fundamental measurement of the phase delay is demonstrated by probing the edge of an as-cleaved silicon wafer in the lateral direction. The measurement results of corner edge profile of an as-cleaved silicon wafer suggest that the proposed method is valid for sensing a position with the resolution of nanometer order.*
Key words: *vibrating microsphere, viscous drag coefficient, laser trapping, probing technique, nano-CMM.*

1. INTRODUCTION

Micro-system technology (MST) including micro-mechanical system, micro-optical system, three-dimensional LSI, MEMS (Micro-Electro-Mechanical System), MOEMS (Micro-Opto-Electro-Mechanical System) is expanding in several directions where complex micro components made of various materials are being realized in addition to the conventional silicon photolithography process as seen in recent development of various three-dimensional micromachining technologies (Groche et al., 2004, Takeuchi et al., 2002, Masuzawa et al., 2002). Moreover, the application fields in the concept of micro engineering (Alting et al., 2003) have been widely spreading in recent years. With these technical trends, the assessment of three-dimensional micromachining accuracy is becoming important more and more because a widening gap between design and implementation is accompanied by a decreasing minimum feature size and increasingly complicated micro components. So, the establishment of assessment technologies for three-dimensional micromachining accuracy is an urgent issue.

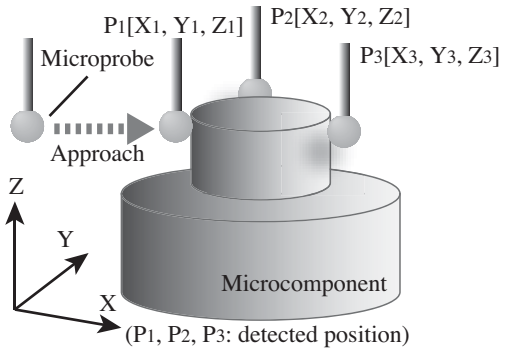

Figure 1: 3D shape measurement of a micro-component using the nano-CMM with a microprobe

To assess dimension, size and other geometrical quantities of micro machined three-dimensional shape based on coordinate metrology with nanometer order accuracy, the nano-CMM (Coordinate Measuring Machine) (Takamasu et al., 1996) is required. The nano-CMM of 1/100 or 1/1000 scale down of a conventional one is proposed to be used for coordinate metrology of micro parts by probing a position, as its concept is show in Figure 1. A microprobe approaches a micro component using a three-dimensional stage system with not only positioning but also moving accuracy of nanometer order, which is calibrated using the international length standard. So, the nano-CMM and its probe are required to satisfy the harsh specifications as shown in Table 1. The target accuracy of less than 50 nm within a 10 mm cubed working volume should be achieved. The probing technique for the nano-CMM is still the key technology, since it is very hard to meet the harsh demands on a position sensing probe with the size of micrometer order and nanometer order resolution. As the microprobe satisfying these requirements for the nano-CMM, we have been developing the laser

Nano-CMM	Measuring Range	10 mm^3
	Resolution	10 nm
	Accuracy	50 nm
Probe	Ball Diameter	10 μm
	Ball Spherisity	10 nm
	Sensitivity	10 nm
	Measuring Force	10^{-5} N

Table 1: Principal performance required to the nano-CMM and the probe with a micro probe sphere

trapping probe (Takaya, Shimizu et al., 1999, Takaya, Takahashi et al., 1999, Takaya et al., 2000) whose principle is based on the single-beam gradient-force optical trap probe (Ashkin et al., 1986) of a micrometer size probe sphere and the vibration probing technique (Nishikawa et al., 2002, Imai et al., 2004, Takaya et al., 2004). As matters relevant to the subject of making the laser trapping probe to be available in manufacturing environment, we focus our argument on the elemental properties as follows. One is trapping a probe sphere in air and the other is decreasing measurement uncertainty concerned with probing.

This paper deals with dynamic properties and position sensing characteristics of a newly developed vibration probing technique. An optically trapped silica particle of 8 μm in air is used as a probe sphere. This has a low spring constant of about 10^{-5} N/m. It is forced to vibrate with several hundreds nanometer amplitude by the laser beam scanning method. In the position sensing probe system, a position sensing detector (PSD) is introduced to detect the back scattered light of He-Ne laser from the vibrating microsphere.

Based on the dynamic model of an optically vibrated microsphere and changing viscous drag coefficient near the surface, the vibrating conditions of the microsphere such as amplitude and phase delay are theoretically analyzed. Probing the edge of an as-cleaved silicon wafer with a crystal surface, it is confirmed that the amplitude and phase delay response change with rapidly increasing viscous drag coefficient near the surface. The position detection principle using the phase delay response for the vibration tuned at the particular frequency is found to be so sensitive as to attain nanometer order resolution. The validity of the position detection principle is verified by measurement of corner edge profile.

2. OPTICALLY TRAPPED MICROPROBE

2.1 Dynamics of an optically trapped micro-sphere

In the vibration probing technique, an optically trapped dielectric particle is used as a probe sphere, which is forced to vibrate based on the nature in dynamics as shown in Figure 2. An optically trapped dielectric particle retains a stable position with the dynamical balance of the gravity force F_g and the trapping force F_t, which is produced by the focused laser beam, as shown in Figure 2(a). When the laser beam is deflected, the trapping force F_t changes with the radiation pressure distribution depending on illumination conditions of the dielectric particle, as shown in Figure 2(b). In this situation, the dielectric particle is accelerated by the resulting force of $F_t + F_g$ in the radial direction and shifts to a deflected beam center from the initial position, as indicated in Figure 2(c). Using this nature in dynamics, an optically trapped dielectric particle can be forced to vibrate with a repeatedly deflected laser beam, that is, a laser beam scan.

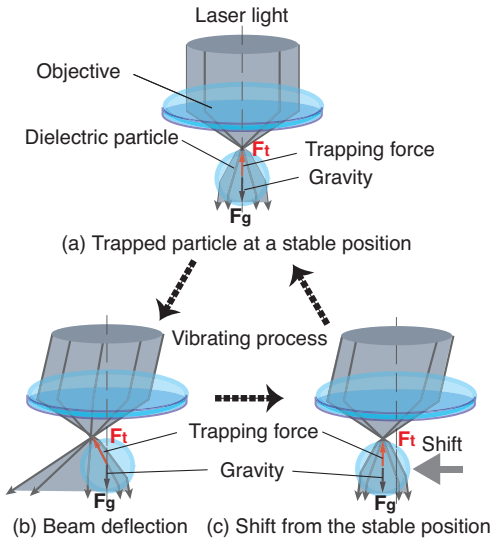

Figure 2: Dynamical behavior of an optically trapped dielectric particle.

2.2 Principle of vibration probing technique

2.2.1 Dynamic model of an optically vibrated particle

Figure 3 shows dynamic properties of a dielectric particle which is optically trapped at a deflected laser beam waist. The particle optically trapped against the forces of gravity F_g is constrained to follow in static situations. When the laser beam is deflected, the particle is accelerated in the lateral direction by the component $F_{st,\,x}$ of the trapping force F_{st} and shifts to the deflected beam center A from the initial position. In this static situation, $F_{st,\,x}$ is

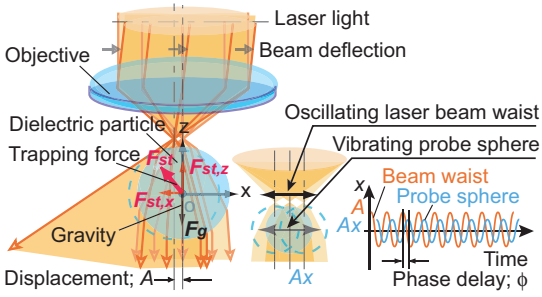

Figure 3: Dynamic properties of a dielectric particle which is optically trapped at a deflected laser beam waist.

given by $F_{st,\,x} = kA$ for a small A, where k is the spring constant in the lateral direction. It is deduced from these dynamic properties that an optically trapped particle can be modeled as a mass placed in a three-dimensional harmonic potential (Friese et al, 1996). When the beam waist is oscillated as $A\sin\omega t$, the force is modulated as $F_{st,\,x}\sin\omega t = kA\sin\omega t$. Then the particle is forced to vibrate by the exciting force $F_{st,\,x}\sin\omega t$ as shown in Figure 3; besides, the motion of the trapped particle is damped by the viscosity of the surrounding atmosphere. According to the Stokes Law,

a microsphere that moves in air at low velocity v undergoes viscous drag Dv, and its viscous drag coefficient D is given by

$$D = 6\pi\eta r \qquad (1)$$

Where r is the radius of the microsphere and η is the dynamic viscosity of the surrounding air. Hence it is governed by

$$m\ddot{x} + D\dot{x} + kx = F_{st,x}\sin\omega t + F(t) \qquad (2)$$

Where $x = A_x \sin(\omega t - \phi)$ is the particle's position in the lateral direction; m, the mass of a particle; $F(t)$, a random force from the air molecules.

In our measurement technique, since a time constant of a lock-in amplifier sets a narrow band, it is possible to detect only the motion associated with this periodicity. So, the contribution of the random force in such a narrow band of frequencies is negligible, that is $F(t)=0$. From Equation (2), the amplitude A_x and the phase delay ϕ of the particle's vibration are obtained as

$$A_x = \frac{k}{\left[\left(k - m\omega^2\right)^2 + D^2\omega^2\right]^{1/2}} A \qquad (3)$$

$$\phi = \cos^{-1}\frac{k - m\omega^2}{\left[\left(k - m\omega^2\right)^2 + D^2\omega^2\right]^{1/2}} \qquad (4)$$

When f_n is a resonant frequency, which is related to the spring constant k by this equation.

$$f_n = \frac{1}{2\pi}\sqrt{\frac{k}{m}} \qquad (5)$$

The dynamic properties of a vibrating probe such as the amplitude response and the frequency response are discussed based on this dynamic model described by these equations

2.2.2 Detection of probe sphere motions using PSD

The probe sphere motions such as the lateral shift and the vibration with the amplitude and the phase delay are precisely detected using a PSD. Figure 4 shows monitoring of the probe sphere motions using the PSD and the principle of position detection. As a light source for trapping a probe sphere, an Nd:YAG laser is used. Oscillating the Nd:YAG laser beam waist, a driving force exerted by a radiation pressure gives a vibration to the probe sphere in the lateral direction. At the same time, the probe sphere is illuminated by a He-Ne laser light, as shown in Figure 4(a). The scattered light by the probe sphere forms a focused light spot on the PSD at a confocal plane. The focused light spot moves on the PSD according with the real motions of the probe sphere. The PSD converts the incident light spot into continuous position signal. The relationship between the currents $X1$ and $X2$ (or $Y1$ and $Y2$) gives the light spot position Ix (or Iy) through the formulas

$$I_{x(y)} = \frac{L_{x(y)}X(Y)_2 - X(Y)_1}{2X(Y)_1 + X(Y)_2} \qquad (6)$$

Where, Lx and Ly is equal to the length of the PSD in the X and Y dimensions respectively (Figure 4(a)). With these

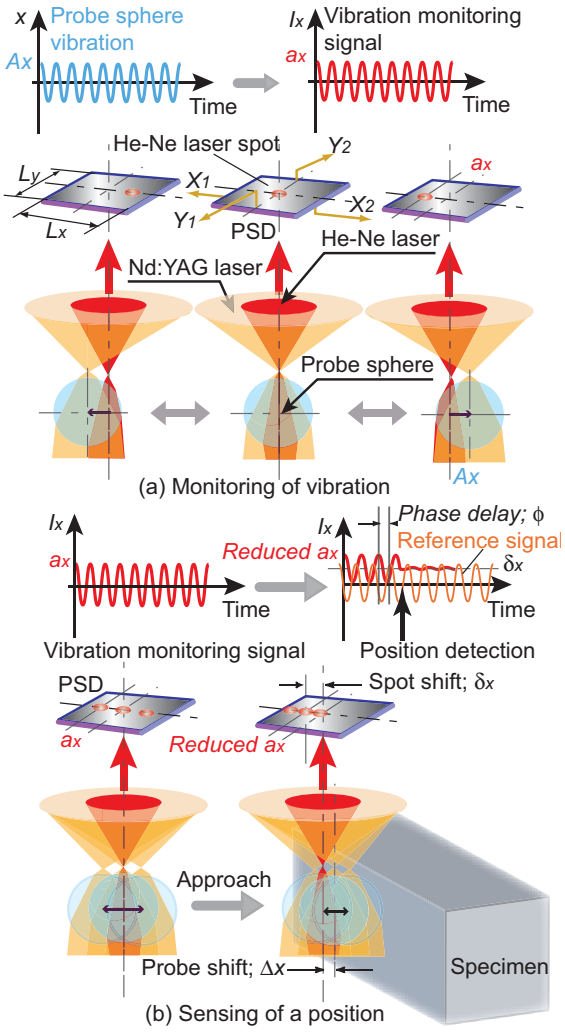

Figure 4: Monitoring of the probe sphere motions using the PSD and the principle of position detection

equations the intensity of the incident light spot does not affect the calculation of the light spot position. The monitoring signals Ix and Iy reflect the probe sphere motions. For example, the position detection signals such

as a response amplitude a_x, a phase delay ϕ and a spot shift δx are extracted from the monitoring signal *Ix,* as indicated in Figure 4(b). Consequently, a three dimensional position on a micro component can be detected based on the change of the position detection signals which are obtained from the monitoring signals of *Ix* and *Iy*.

3. MICROPROBE SYSTEM USING PSD

3.1 Microprobe system setup

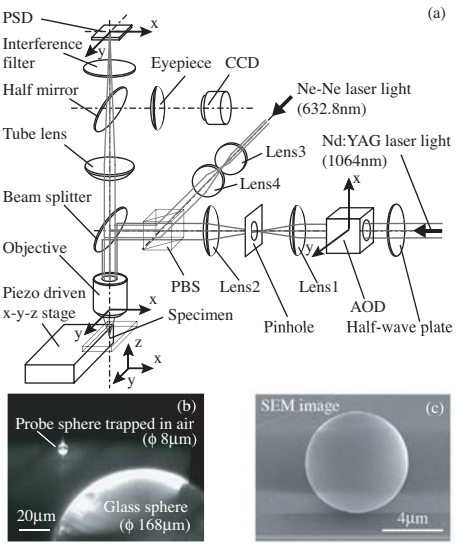

Figure 5: Experimental setup. (a) Schematic diagram of the position sensing probe system. (b) Microscopic image of the optically trapped probe sphere in air. (c) SEM image of a microsphere.

Schematic diagram of the position sensing probe system based on the vibration probing technique is illustrated in Figure 5(a). The experimental setup consists of three functional components such as an optical system for trapping and vibrating a probe sphere, a detection system for monitoring the vibrating conditions and an imaging optics for microscopic observation and a stage system. The linearly polarized light for optical trap with the wavelength of 1064 nm is emitted from an Nd:YAG laser (818ST Q-SW, Lee Laser). The laser beam is scanned by an acousto-optic deflector (AOD) with two axes. The scanning angle is adjusted using relay lens components of the lens1 and lens2 with the focal lengths of 128.2 mm and 256.4 mm, respectively. To minimize the loss of the laser power, the AOD is positioned at an optical conjugate plane of the back focal plane of an objective. After passing through a polarizing beam splitter (PBS), it is deflected by a beam splitter and focused by the objective with N.A. of 0.95 on a silica particle with the diameter of 8.0 mm used as a probe sphere. The beam is oscillated with the desired frequency and amplitude at the focal plane. It is possible to maintain the probe sphere stably by switching the Nd:YAG laser light emission from the pulse mode to the CW mode with lower power than 100 mW. In the same manner, the He -Ne laser light with the wavelength of 633 nm is collimated by using the lens3 and lens4 with the focal lengths of 20 mm and 80 mm, respectively. It joined with the Nd:YAG laser light concentrically at the PBS to illuminate the optically trapped probe sphere. The backscattered He -Ne laser light from the probe sphere is detected using a PSD (Hamamatsu, S5990-01) placed in the confocal arrangement after passing through an interference filter which eliminates the Nd:YAG laser light. The PSD converts the incident light spot into continuous position signal. The vibrating conditions are monitored by the voltage output signal from the PSD which is sent to a lock-in amplifier and a PC. The signal from PSD and the reference signal driving the AOD together are analyzed to measure the probe sphere motions. The probe sphere is positioned relatively to a specimen, which is fixed on a XYZ-sample stage driven by PZT actuators with the

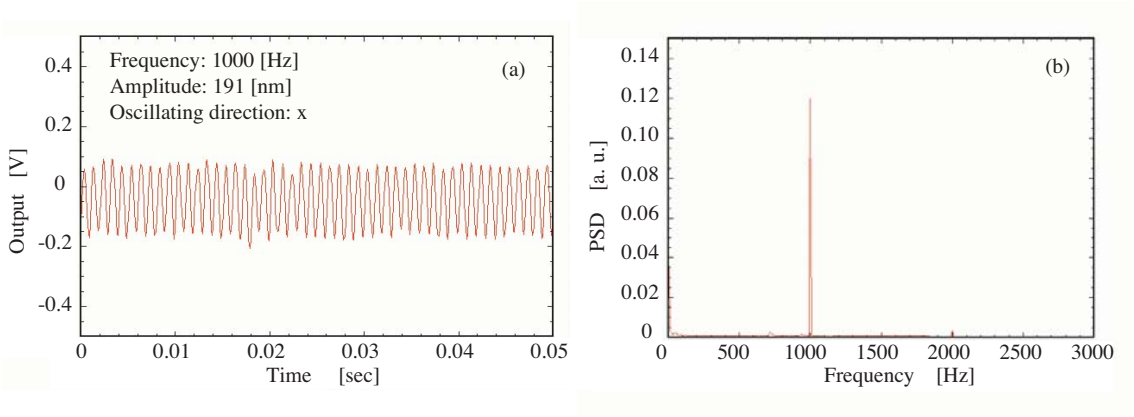

Figure 6: Vibrating condition signal of the microsphere obtained from the backscattered light which is detected using the PSD. (a) The time domain signal of vibration in the x-direction. (b) Power spectral density.

positioning accuracy of 5 nm. Using this experimental setup a microsphere can be optically trapped in air as shown in a microscopic image (Figure 5(b)). The

microsphere has enough high sphericity to use as a probe sphere as indicated in a SEM image (Figure 5(c)).

3.2 Measurement of dynamic properties

A microsphere is experimentally driven by the laser beam oscillation in the transverse direction with trapping in air. Giving the laser beam oscillation at the amplitude of 191 nm and the frequency of 1000 Hz, the vibrating condition signal of the microsphere is obtained from the backscattered light which is detected using the PSD as shown in Figure 6. A strong response peak at the frequency of 1000 Hz in the power spectrum (Figure 6(b)) is confirmed by employing FFT analysis of the time domain signal (Figure 6 (a)), which is coincident with the frequency of the laser beam oscillation.

In order to analyze dynamic properties of a vibrating microsphere, the amplitude response and frequency response are measured. Figure 7 illustrates measurement results of the amplitude and frequency for the vibrating probe in the x- and y-direction. The xy-coordinate system is defined in Figure 5. Figure 7(a) shows the amplitude response for increasing amplitude of the laser beam oscillation ranging from 24 nm to 542 nm at the frequency of 1000 Hz. Measurement results show that vibrating amplitude of the microsphere is directly proportional to the given amplitude by the laser beam oscillation for both of the x- and the y-direction. Figure 7(b) indicates the frequency response ranging from 50 Hz to 3 kHz at the amplitude of 191 nm and the least squares fitted curve. The fitting is performed using Equation (3) and the constant values according to the experimental conditions: the radius of the probe sphere r = 4.0 X 10^{-6} m, the mass of the probe sphere m=5.0X10^{-13} kg, η= 1.81 X 10^{-5} Pa•s of the dynamic viscosity of ideal gas at 293 K. Substituting the resonant frequency of f_n = 1780 Hz for the x-direction and f_n = 1670 Hz for the y-direction obtained from the least-squares fitting into Equation (5), the lateral spring constants of K_x and K_y are estimated 6.3 X 10^{-5} N/m and 5.5 X 10^{-5} N/m, respectively. These measurement results make it clear that using the linearly polarized light the spring constant K_y is smaller than K_x. This is explained by the fact that when an optically trapped microsphere is illuminated by the laser light linearly polarized in the x-direction, the trapping force in the y-direction is smaller than that in the x-direction (Wright et al., 1994).

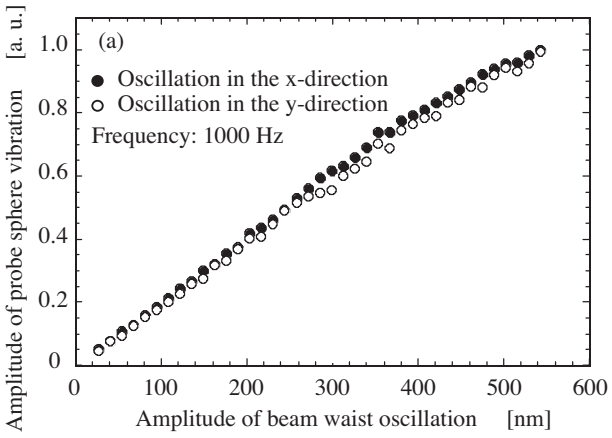

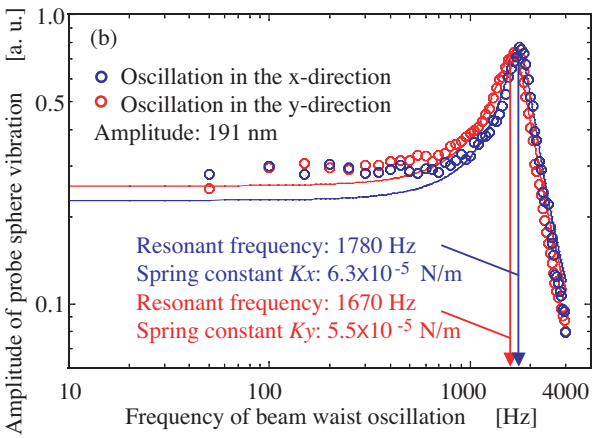

Figure 7: Measurement results of the amplitude and the frequency for the probe vibrating in the x-and y-direction. (a) The amplitude response ranging from 24 nm to 542 nm. (b) The frequency response ranging from 50 Hz to 3 KHz.

4. POSITION SENSING EXPERIMENTS

4.1 Dynamics properties in probing

The drag force acting on a vibrating microsphere is taken to be constant when a microprobe is moving in free space, that is, the viscous drag coefficient D in the differential equation given by Equation (1) is a constant wherever the microprobe are. However, the microprobe for the nano-CMM approaches a specimen's surface in measurement of a position. Especially, to sense a nano-position approaching, the microsphere moves not far away from the specimen's surface but very close to it. Such the

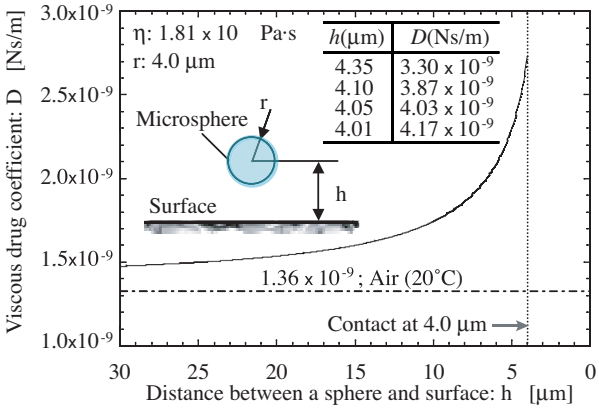

Figure 8: The theoretical curve of viscous drag coefficient changing with the distance between the center of the microsphere and the surface

microprobe is affected by the drag force changing with distance from a surface in vibrating condition because there is no treating viscous drag coefficient as a constant value. When an atmosphere surrounding a microsphere is incompressible and Reynolds number is sufficiently small, this fluid behaves in accordance to the Stokes equation. Taking this under consideration D is corrected by the factor P of the boundary condition correction for specimen's surface and given by,

$$D = 6\pi\eta r \quad (1+P) \qquad (7)$$

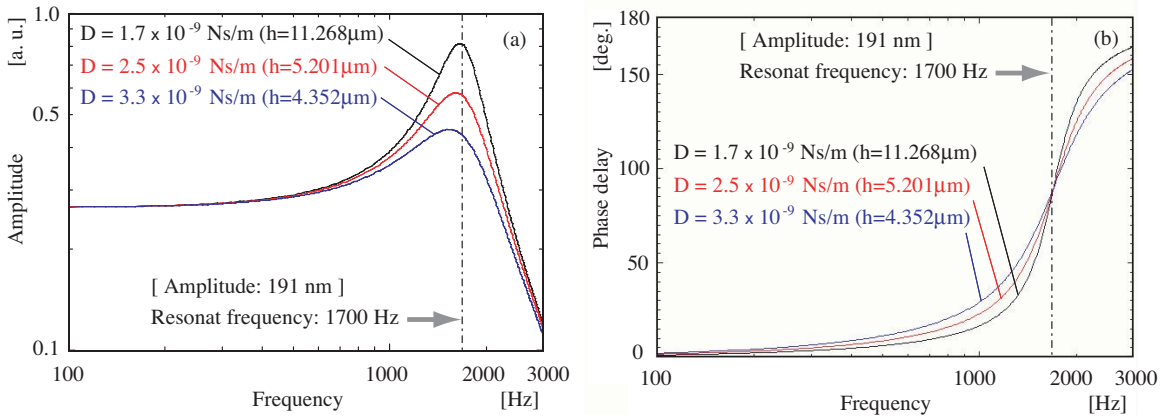

Figure 9: The theoretical curve of the amplitude and the phase delay for different viscous drag coefficients. (a) The amplitude response for the frequency ranging from 100 Hz to 3 KHz. (b) The Phase delay response for the frequency

P is obtained as the function of the radius of the microsphere r and the distance h between the center of the microsphere and the surface (Happel & Brenner, 1965),

$$P = \frac{1}{\left\{1 - \frac{9}{16}\left(\frac{r}{h}\right) + \frac{1}{8}\left(\frac{r}{h}\right)^3 - \frac{45}{256}\left(\frac{r}{h}\right)^4 - \frac{1}{16}\left(\frac{r}{h}\right)^5\right\}} - 1 \qquad (8)$$

Figure 8 shows the theoretical curve of viscous drag coefficient D changing with h for r = 4.0 X 10^{-6} m and η= 1.81 X 10^{-5} Pa•s of the dynamic viscosity of ideal gas at 293 K. This reveals drastically increasing viscous drag coefficients with decreasing distance from the surface, especially when the microsphere moves within 10 μm of a surface. Approaching within a clearance of 350nm between the microprobe's surface and the surface, the viscous drag coefficient varies from 3.30 X 10^{-9} to 4.17 X 10^{-9} more than three times as many as that of air at 20°C. In consequence of this, a position with nanometer order accuracy is measurable by detecting the increase of the viscous drag coefficient.

To investigate the position sensing method based on the viscous drag coefficient change, the numerical analyses of the vibrating conditions of the microsphere such as amplitude and phase delay for changing frequency are performed using Equation (3) and (4). Figure 9 shows the theoretical curve of the amplitude and phase delay for different viscous drag coefficients. The amplitude and phase delay are calculated for the frequency ranging from 100 Hz to 3000 Hz. The amplitude at the resonant frequency of 1700 Hz decreases gradually with increasing viscous drag coefficient. On the other hand, the phase delay is constant at the resonant frequency, but increases remarkably with increasing viscous drag coefficient near the frequency of 1000 Hz and decreases near 3000 Hz also. Consequently, the position sensing based on decreasing amplitude at the resonant frequency and changing phase delay near 1000 Hz or 3000 Hz is effective.

4.2 Position sensing resolution

In order to verify the validity of the position detection principle based on the vibrating condition of the probe,

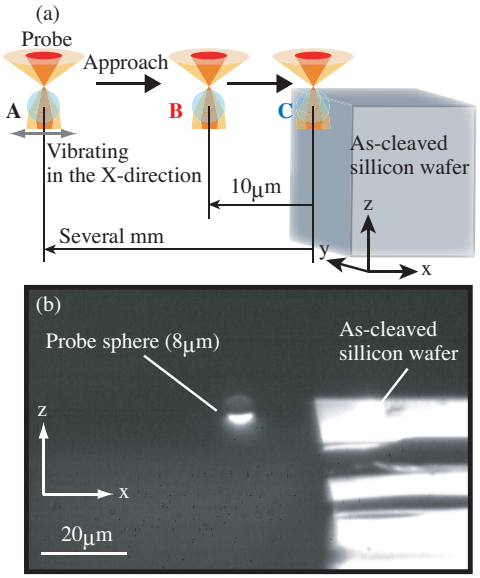

Figure 10: Probe approaching the crystal surface of an as-cleaved silicon wafer. (a) Schematic diagram of measurement positions. (b) Microscopic image.

measurement of frequency responses with approaching a specimen is carried out. The probe is brought close to the edge of an as-cleaved silicon wafer in the lateral direction, which has a crystal surface with the smoothness of atomic level. As shown in Figure 10(a), the probe starts from the initial location A of several mm from the surface and the frequency response is measured at A, B of 10 μm from the surface and C almost contact with the surface. The microscopic image in measurement is indicated in Figure 10(b). The microsphere is forced to vibrate in the x-direction at the initial amplitude of 191 nm and the frequency of 1700 Hz, since the vibration toward the surface is expected to emphasize the change of viscous drag coefficient by the damping effect that is brought by repetition of compressing and expanding the thin air film formed between the microsphere's surface and the specimen's surface. This meets the demand on that the advantageous performance for a position detection probe is to enable it to sense a specimen at a location of several micrometers from a surface also. Figure 11(a) and (b) show measurement results of the amplitude and phase delay for the frequency ranging from 100 Hz to 3 KHz. K_A, K_B, K_C and D_A, D_B, D_C are spring constants and viscous drag coefficients at A, B and C which are obtained as the least-squares fitting parameters. Whereas the increase in the viscous drag coefficient with decreasing distance from the surface confirms theoretical expectations, the measured viscous drag coefficients of D_A, D_B and D_C does not comply with theory. This is because of the influence of the damping effect and the difference of the dynamic viscosity of air depending on temperature.

To confirm measurement accuracy of nanometer order the position detection method based on changing phase delay near the surface is examined. The microsphere being forced to vibrate with the amplitude of 191 nm and the frequency of 950 Hz approaches the specimen's surface in the x-direction. The vibration is tuned to this frequency because the phase delay is sensitive to the change of viscous drag coefficient at this frequency in the vicinity of the surface, as shown in Figure 10(b). Relative positioning between the probe and the specimen is done by moving the sample stage at 25 nm intervals within about 1 μm distance from the surface. Figure 12 illustrates the position sensing by lateral probing of the crystal surface of the as-cleaved silicon wafer edge. The phase delay increases according to changing of the viscous drag coefficient close to the specimen's surface. The resolution of position detection is evaluated with the ratio of the standard deviation of 0.59 degree to the sensitivity which is defined by the inclination of the phase delay response curve. The inclination is obtained 25.74 degree/μm from the least squares fitting line of data neighboring the position detection threshold of 75 degree. So, the vibrating microprobe is effective for detecting a position with the position detection resolution of finer than 23 nm.

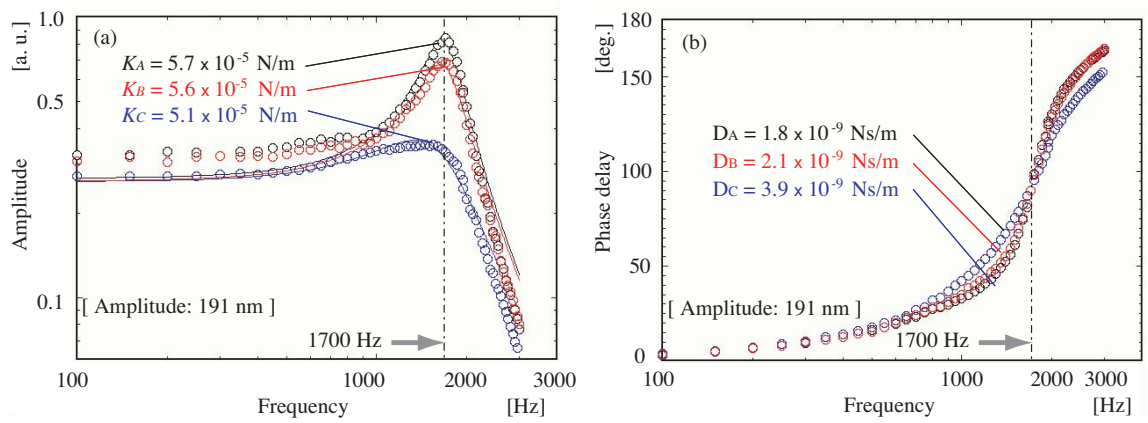

Figure 11: Measurement of the amplitude and the phase delay for the vibrating probe approaching the crystal surface in the x-direction. (a) The amplitude response for the frequency ranging from 100 Hz to 3 KHz. (b) The Phase delay response for the frequency ranging from 100 Hz to 3 KHz.

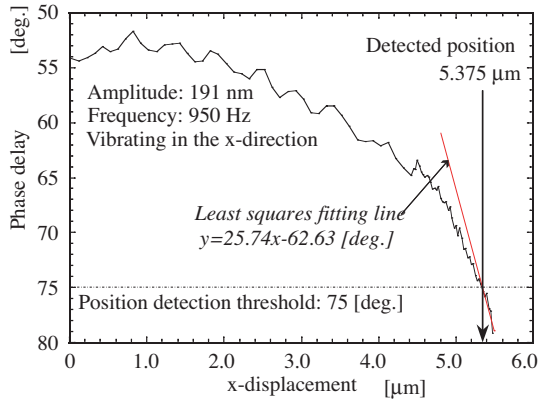

Figure 12: Position sensing based on the phase delay change by probing the crystal surface of an as-cleaved silicon wafer.

4.3 Measurement of corner edge profile

Figure 13 illustrates Measurement results of corner edge profile of the crystal surface of an as-cleaved silicon wafer. Lateral probing is performed in normal direction to

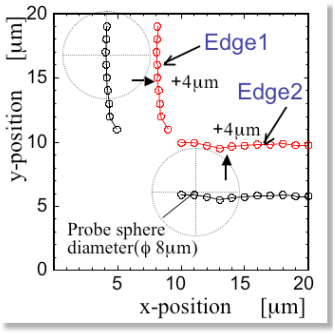

Figure 13: Measurement results of corner edge profile of the crystal surface of an as-cleaved silicon wafer

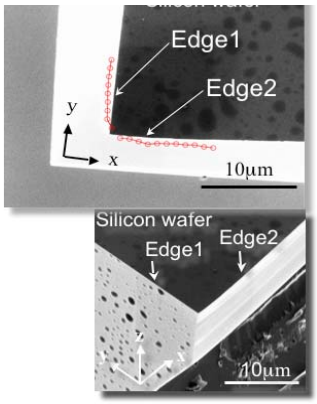

Figure 14: SIM (Scanning Ion-beam Microscope) images of corner edge of the crystal surface of an as-cleaved silicon wafer and probing points plot.

the surface of the as-cleaved silicon wafer edge. The edge profile is obtained by compensating the probe sphere radius of 4 μm. Figure 14 shows SIM (Scanning Ion-beam Microscope) images of corner edge of the crystal surface of an as-cleaved silicon wafer. Measured corner edge profile is indicated on the SIM image. The measurement results suggest that the optically vibrated microprobe is effective for detecting a position with the resolution and useful for the probing method for the nano-CMM.

5. CONCLUSION

As a position detection probe for the nano-CMM, the dynamic properties and a novel principle of position sensing of the vibrating microsphere is presented. The dynamic model of an optically vibrated microsphere is discussed based on a mass in a three-dimensional harmonic potential with taking account of viscous drag force in the surrounding atmosphere. Both results from numerical and experimental analyses reveal drastically increasing viscous drag coefficients with decreasing distance from the surface, especially when the microsphere moves within 10 μm from the surface. To verify the validity of the principle of position sensing, the phase delays are measured by probing the edge of an as-cleaved silicon wafer in the lateral direction, which has a crystal surface with the smoothness of atomic level. In this experiment, the vibration is tuned to the frequency of 950 Hz because the phase delay is sensitive to changing viscous drag coefficient in the vicinity of the surface at this frequency. The measurement results of the corner edge profile suggest that the optically vibrated microprobe is useful as probing technique for the nano-CMM.

6. REFERENCES

Alting, L.; Kimura, F.; Hansen, H.N. and Bissacco, G. (2003). Micro engineering, *Annals of the CIRP*, Vol. 52/2, pp. 635-657.

Ashkin, A; Dziedzic, J. M.; Bjorkholm, J. E. and Chu, S. (1986). Observation of a single-beam gradient force optical trap for dielectric particles, *Optical Letters*, Vol. 11, pp. 288-290.

Friese, M. E. J.; Truscott, A. G.; Dunlop, H. R. and Heckenberg, N. R. (1996), Determination of the force constant of a single-beam gradient trap by measurement of backscattered light, *Applied Optics*, Vol. 35/36, pp. 7112-7116.

Groche, P. and Schneider, R. (2004). Method for the optimization of forming presses for the manufacturing of micro parts, *Annals of the CIRP*, Vol. 53/1, pp. 281-284.

Happel, J. and Brenner, H. (1965). Low Reynolds number hydrodynamics with special applications to particulate media, *Prentice-Hall, NJ*, p. 327.

Imai, K.; Takaya,Y., Miyoshi, T., Ha, T. and Kimura, K. (2004). Position sensitivity of micro probe with transverse vibration using optical trap, *Proc. of Int. Symposium on Photonics in Measurement*, pp. 277-284.

Masuzawa, T.; Okajima, K.; Taguchi, T. and Fujino, M. (2002). EDM-Lathe for micromachining, *Annals of the CIRP*, Vol. 51/1, pp. 355-358.

Nishikawa, M.; Takaya, Y., Takahashi, S., Uekita, M. and Miyoshi, T. (2002). Probing technique for microparts using optically trapped particle by annular beam, *Proc. of Int. Symp. on Photonics in Meas.*, pp. 103-108.

Takamasu, K.; Ozawa, S; Asano, T.; Suzuki, A.; Furutani, R. and Ozono, S. (1996). Basic concepts of nano-CMM, *Proc. of the Japan-China Bilateral Symposium on Advanced Manufacturing Engineering*, pp. 155-158.

Takaya,Y.; Imai, K.; Ha, T. and Miyoshi, T. (2004). Vibrational probing technique for the nano-CMM based on optical radiation pressure control, *Annals of the CIRP*, Vol. 53/1, pp. 421-424.

Takaya, Y.; Shimizu, H.; Takahashi, S. and Miyoshi, T. (1999). Fundamental study on the new probe technique

for the nano-CMM based on the laser trapping and Mirau interferometer, *Measurement*, 25, 9-18.

Takaya, Y.; Takahashi, S. and Miyoshi, T. (2000). Nano-positional detection using laser trapping probe for micro parts, *Proc. of ASPE 2000 Annual Meeting*, pp. 584-587.

Takaya, Y.; Takahashi, S.; Miyoshi, T. and Saito K. (1999). Development of the nano-CMM probe based on laser trapping technology, *Annals of the CIRP*, Vol. 48/1, pp. 421-424.

Takeuchi, Y.; Maeda, S.; Kawai, T. and Sawada, K. (2002). Manufacture of multiple-focus micro Fresnel lenses by means of non-rotational diamond grooving, *Annals of the CIRP*, Vol. 51/1, pp. 343-346.

Wright, W. H.; Sonek, G. J. and Berns, M. W. (1994). Parametric study of the forces on microspheres held by optical tweezers, *App. Opt.*, Vol. 33/9, pp. 1735-1748.